MICHIGAN STATE
UNIVERSITY

National Superconducting Cyclotron Laboratory

# $^4$He + $^4$He ELASTIC SCATTERING AT 280 AND 620 MeV

**K.A.G. RAO, A. NADASEN, D. SISAN, W. YUHASZ , D. MERCER, SAM M. AUSTIN, P.G. ROOS, R.E. WARNER**

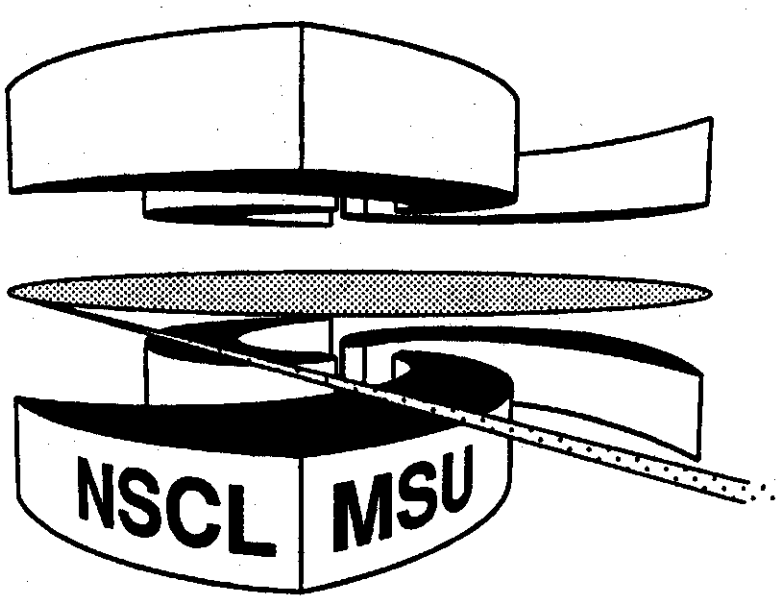


**MSUCL-1148** **APRIL 2000**

# $^4$He + $^4$He Elastic Scattering at 280 and 620 MeV

K.A.G. Rao, A. Nadasen, D. Sisan, W. Yuhasz

*Department of Natural* Sciences, University *of Michigan, Dearborn, Michigan 48128-1491*

D. Mercer

*Department of* Physics, *University* of *Colorado, Boulder, Colorado*

Sam M. Austin

National *Superconducting Cyclotron Laboratory and Department of* Physics and *Astronomy,* Michigan *State University, East* Lansing, Michigan *48824-1321*

P.G. Roos

*Department of* Physics, University of Maryland, *College Park, Maryland* 20742

R.E. Warner

*Department of Physics, Oberlin College, Oberlin, Ohio* 44074

(Draft: April 20, 2000)

## Abstract

Differential cross sections for the elastic scattering of $^4$He from $^4$He have been measured at 280 and 620 MeV. The data exhibit systematic energy dependence when compared with measurements at lower energies. Optical model analysis indicates that the Woods-Saxon potential fails to reproduce the large angle data. Satisfactory fits are obtained by adding a Woods-Saxon squared form factor to the real central potential.

PACS number(s): 25.10.+s, 25.55.Ci

## I. INTRODUCTION

For several decades there has been considerable interest in the interaction between two $\alpha$-particles. First, such a relatively simple system provides the opportunity for carrying out fundamental calculations of the reaction. Second, the zero spin-isospin nature and the large binding energy of the $\alpha$-particle make it an important constituent in the cluster model [1]. It is well known that light cluster nuclei like $^{6,7}$Li, $^{9}$Be, $^{12}$C, and $^{16}$O contain $\alpha$-particle substructures, as evidenced by $\alpha$-transfer and $\alpha$-knockout reactions [2–6]. Further, $\alpha$-decay of heavy nuclei provides evidence that $\alpha$-clusters may pre-exist in the surface of these nuclei. Calculations for such models rely heavily on accurate knowledge of the $\alpha$-nucleus interaction, the simplest of which is the $\alpha$-$\alpha$ interaction.

There have been several theoretical [7–9] and experimental studies [10–14] of the $\alpha$-$\alpha$ system. At least three different approaches have been taken to interpret $\alpha$-$\alpha$ elastic scattering. Darriulat et al. [12] analyzed the phase shifts extracted from data ranging from 50 to 120 MeV using an energy-independent, but strongly $l$-dependent, potential together with a repulsive core. This calculation ignores possible bound states which are forbidden by the Pauli principle. Then the phase shifts, $\delta_l$, are all zero at zero energy, causing the $l = 0$ and $l = 2$ phase shifts to become negative at higher energies. This behavior of the partial waves naturally results in a repulsive core which arises from nonlocal terms due to the Pauli exclusion principle. In a second approach, Czyz and Maximon [15] have calculated $\alpha$-$\alpha$ elastic scattering in the Glauber approximation [16]. The test of the Glauber model can be much more effective for $\alpha$-$\alpha$ elastic scattering than for nucleon-nucleus scattering because of multiple scattering. Since more than one nucleon in the projectile can collide with each target nucleon, additional multiple scattering amplitudes are generated. These theoretical predictions are applicable at very high energies. Therefore data at energies beyond 1 GeV may be needed to test the Glauber model. A third approach has been suggested by Swan [17]. In elastic scattering of complex systems, certain states are forbidden by the Pauli exclusion principle. Swan argued that the forbidden states should be included in Levinson's

theorem. Then the phase shifts at zero energy, $\delta_l(0)$, will be determined by both the number of observed bound states and the number of forbidden states. As a consequence Neudatchin [9] employed a deep $l$-dependent attractive local potential of the Woods-Saxon form which contains the $1s$, $2s$, and $1d$ forbidden states. Then at zero energy the phase shifts are $\delta_0(0) = 2\pi$, $\delta_2(0) = \pi$, and $\delta_{l>2}(0) = 0$. The $\delta_0$ and $\delta_2$ phase shifts continue to decrease with energy but always remain positive, thus removing the necessity for a repulsive core. The phase shifts extrapolate smoothly to zero at high energies.

There are abundant $\alpha + \alpha$ elastic scattering data below 200 MeV for testing of the different approaches which have been postulated. The repulsive-core potential [12] has been supported by data up to 120 MeV. However, the energy dependence of the potential without a repulsive core [9] and its development towards the Glauber approximation [16] have not been verified experimentally for sufficiently high energies because very few $\alpha$-$\alpha$ elastic scattering data exist beyond 200 MeV. Measurements with large uncertainties over limited angular ranges are available at 650 and 850 MeV [18]. The data at 900 MeV [19] have poor statistical accuracy and large angular acceptances. Therefore we have measured, and report in this paper, $\alpha + \alpha$ elastic scattering at 280 MeV and 620 MeV covering the full angular range up to 90° center of mass. Our goal is to provide high quality data over the full angular range for energies beyond 200 MeV so that the various theoretical postulates can be evaluated. Our data will also provide energy dependence for the $\alpha$-$\alpha$ interaction for a range of energies extending to three times that of previous investigations.

In section II, we describe the experimental procedure. We discuss the data reduction and results of our measurements in section III. The optical-model analyses of the data are presented in section IV. Finally, concluding remarks are made in section V.

## II. EXPERIMENTAL PROCEDURE

The measurements were made with $\alpha$-particle beams produced by the K1200 cyclotron of the National Superconducting Cyclotron Laboratory at Michigan State University. The

beams were momentum analyzed with the double dipole analyzing system of the A1200. The uncertainty in the beam energy was estimated to be less than 0.2% from the cyclotron and A1200 parameters. The energy resolution of the beam was estimated to be better than 0.1%. The beam was directed to the center of a cylindrical scattering chamber 2.3 m in diameter and 3.0 m long. The beam line elements were adjusted for minimal steering of the beam as observed on a scintillator at the center of the chamber. The beam spot at the center of the target was 2 mm wide and 4 mm high. The beam currents ranged from a fraction of a nA to ~20 nA depending on the angle of measurement and were controlled in order to minimize pile-up effects and dead time in the detection system.

The target for the 620 MeV measurements was high purity $^4$He gas contained in a 12 cm diameter gas cell located at the center of the evacuated scattering chamber. The gas was maintained at a slightly higher pressure (806 torr) than one atmosphere and allowed to flow slowly through the cell to ensure that the target did not become contaminated. The scattered particles were detected with three detector telescopes separated by 5°. Each telescope consisted of a double slit system which defined the target length and solid angle, followed by a 1 mm surface barrier silicon detector and a 10 cm deep NaI(T$l$). The silicon detectors were calibrated using a $^{228}$Th alpha source and the NaI detectors were calibrated with forward angle $\alpha$-$\alpha$ elastic scattering. This system had an overall energy resolution better than 2%. A similar set of three telescopes was used as monitors. The measurements were made by moving the telescopes in 5° steps. Measurements with the most forward telescope (TEL1) ranged from 10° to 45°, while those with TEL3 ranged from 20° to 55°. This provided sufficient overlap between the two telescopes for cross checking their measurements. The Si detector in TEL2 failed and no data were extracted from it.

For the 280 MeV experiment, a novel technique of filling the entire chamber with $^4$He gas was used, thus eliminating the traditional gas cell. Detector telescopes consisting of two position sensitive silicon strip detectors were used to define the target length and the detection solid angle. This system produced higher yields because longer target lengths could be selected which would otherwise be limited by the size of the gas cell, resulting in

improved statistics at the sacrifice of some angular resolution.

The detector signals were processed using conventional fast-slow electronics. The data were written event by event on magnetic tapes for subsequent detailed analysis. During the experiment one- and two-dimensional arrays were created on-line to monitor deadtime, pile-up effects, gain shifts and general problems associated with the operation of the detection system.

## III. DATA REDUCTION

The event tapes were replayed off-line, and one- and two-dimensional histograms were created for each angle of measurement. A two-dimensional contour plot of $\Delta$E vs. E showed clean separation between $\alpha$-particles and $^3$He. A window around the $\alpha$-particles was used to gate the one-dimensional total energy spectrum, thus selecting the energy distribution of $\alpha$-particles. This spectrum displayed a single peak. At each angle the position of this peak was at the energy predicted by the two-body kinematics for $\alpha + \alpha$ elastic scattering at 280 and 620 MeV. The area under the $\alpha$ peak was extracted and the differential cross section was calculated using the equation

$$d\sigma/d\Omega = [(22.1 N Z_p T)/(\Omega Q Z_{eff} P)]$$

where $N$ = number of counts under the peak. $Z_p$ (= 2) is the atomic number of the projectile, $T$ is the Kelvin temperature of the target and $P$ is its pressure in torr. $Q$ is the total beam charge (in nC) collected in the Faraday cup. $\Omega$ (in msr) and $Z_{eff}$ (in m) are the solid angle and effective target length respectively defined by the double-slit system.

The cross sections were calculated using the above formula and converted into the center of mass frame using relativistic kinematics. Fig. 1 shows the cross sections plotted as a function of center-of-mass angle. Also shown are cross sections for 100, 160, 198, and 650 MeV. The 280 MeV data (solid squares) follow the trend of the lower energy data. The cross sections peak at the very forward angles, decrease steadily until a minimum is reached near 80°, followed by a backward rise to a maximum at 90°. The magnitudes of the cross sections

also follow the trend set by the lower energy data. Overall the 280 MeV cross sections are slightly smaller than those at 198 MeV. The 620 MeV cross sections (solid circles) are much lower at the forward angles, being about two orders of magnitude lower than the 280 MeV data. However, this discrepancy is less apparent at the larger angles and they are in excellent agreement over the limited angular range of the 650 MeV data. The larger decrease in cross section beyond 280 MeV may be attributed to loss of flux in the elastic scattering channel resulting from the onset of pion production.

## IV. OPTICAL-MODEL ANALYSIS

The data were analyzed using the optical model code SNOOPY8 which properly anti-symmetrizes the two identical bosons, resulting in only even partial waves in the partial wave decomposition of the scattering amplitudes. The conventional non-relativistic Schrödinger formulation of elastic potential scattering was employed, with the inclusion of relativistic kinematics. Initially, six-parameter real and imaginary volume central potentials together with a Coulomb potential were included in the analysis. The potential used was

$U(r) = U_c(r, r_c) - Vf(r, r_o, a_o) - iW_v f(r, r_w, a_w)$

where $f(r, r_x, a_x)$ is the Woods-Saxon form factor $\left(1 + \exp[(r - r_x A_t^{1/3})/a_x]\right)^{-1}$ and $U_c(r, r_c)$ is the Coulomb potential due to a uniform sphere with charge equal to that of the target nucleus and radius $r_c A_t^{1/3}$. The mass number, $A_t$, was 4, and this convention is referred to as the light-ion convention. Use of the heavy-ion convention, $R_x = r_x(A_p^{1/3} + A_t^{1/3})$, changes the value of the parameter, $r_x$, but retains the total central potential in its entire form.

The program facilitated searches on any combination of parameters in order to minimize $\chi^2$, defined by

$\chi^2 = (1/N) \sum_{i=1}^{N} \left(\sigma(\Theta_i)^{calc} - \sigma(\Theta_i)^{expt}\right) / \left(\Delta\sigma(\Theta_i)\right)^2$

where $N$ is the number of degrees of freedom and $\sigma(\Theta_i)^{calc}$ is the $i$th calculated cross section. $\sigma(\Theta_i)^{expt}$ and $\Delta\sigma(\Theta_i)$ are the corresponding experimental cross section and its

relative uncertainty, respectively. Starting parameters were taken from the results of the 160 and 200 MeV [14,20] analyses. Initial searches were carried out with various combinations of two parameters, while keeping the others fixed. After minimizing $\chi^2$, three-parameter searches were made. The number of parameters in the searches was continually increased until final searches were made on all six parameters.

The fits to the data were unsatisfactory. The calculations significantly underestimated the large angle cross sections for both energies, as shown by the dashed lines in Figs. 2 and 3. In order to verify that the potentials obtained did not belong to a wrong ambiguous family, grid searches were made. The strength of the real potential, V, was gridded in 5 MeV steps from 5 MeV to 600 MeV, while searching on the other five parameters. No additional minimum in $\chi^2$ was found. Variation of the normalization, combined with grid searches, also failed to improve the fit to the data.

At lower energies [14,20] a combination of two Woods-Saxon potentials were used for the real part of the interaction to provide more flexibility to the shape of the potential. A similar technique was adopted here. However, our code did not have the capability of employing two Woods-Saxon potentials. We therefore used the sum of a Woods-Saxon and a Woods-Saxon-squared potential. For the imaginary potential a three-parameter Woods-Saxon form was retained. The nine parameter search resulted in a significant improvement in the fit, as shown by the solid lines in Figs. 2 and 3. The derived parameters are given in Table I. The shape of the real potential, shown in Fig. 4, for both the 280 and 620 MeV data, is very similar to those obtained at lower energies. A deep potential is observed in the interior, decreasing to near zero at about 3 fm., followed by a weak component that has a longer range. For 280 MeV the total potential decreases to zero at about 7 fm., whereas for 620 MeV the weak potential seems to have a longer range.

The volume integral per nucleon pair of the real potential has values of 367 and 180 MeV fm$^3$ for the 280 and 620 MeV data, respectively. These volume integrals are plotted, together with those derived at lower energies, in Fig. 5 (solid dots) as a function of beam energy, which shows an interesting energy dependence of the potentials. The volume integrals of

the real potential show a linear dependence on the incident energy of the form

$J_R(E) = J_R(0) - \beta E$

with $J_R(0) = 480$ MeV$fm^3$ and $\beta = 0.48\ fm^3$. This implies that the volume integral of the real potential becomes repulsive beyond 1 GeV, or 250 MeV/nucleon. This is much lower than the potentials for heavier nuclei, which have been estimated to change sign in the 600-800 MeV/nucleon region.

This rapid decrease in the volume integral of the $\alpha$-$\alpha$ real potential may be attributed to the tightly-bound nature of the $\alpha$-particle as well as the limited number of reaction channels available for this system, both of which result in decreased reaction events. This explanation is supported by the imaginary volume integrals, which increase to a maximum value at an energy of about 150 MeV and then show a slow decrease (open circles in Fig. 5). In the framework of the optical model potential, a reduction in the imaginary potential causes a quenching of the real potential.

An attempt was also made to analyze the data in terms of the formalism of Darriulat et al. [12]. In this regard, a short-range hard-core repulsive potential was added to the Woods-Saxon real potential. Searches with several different starting parameters did not produce any acceptable fit to the data. Searches on the range of the repulsive potential resulted in the range going to zero, with the resulting parameters being similar to those of the six parameter fit obtained in the initial calculations.

## V. CONCLUSION

We have made measurements of the elastic scattering of $\alpha$-particles from $^4$He at bombarding energies of 280 and 620 MeV. The angular distribution of the 280 MeV differential cross sections exhibits behavior similar to those at lower energies showing a smooth fall-off with angle to a minimum at about 80°, followed by a backward rise peaking at 90°. The 620 MeV cross sections show similar fall-off at the forward angles, but have no discernible structure beyond 80°. Also the forward angle cross sections are somewhat lower than the

trend set by the lower energy data. Nevertheless the magnitude of the large angle cross sections are in agreement with previous measurements at 650 MeV.

The optical-model analyses with a six parameter Woods-Saxon potential cannot reproduce the large angle cross sections. A sum of a Woods-Saxon potential and a Woods-Saxon-squared potential provides a much superior fit to the data. Thus the interaction between two $\alpha$-particles seems too complicated to be represented by a simple Woods-Saxon potential. The shape of the total real potential suggests that there may be two components to the $\alpha$-$\alpha$ interaction which could be due to the interplay between a long range and a short range interaction. Because of the tight binding and small size of these nuclei, as the impact parameter decreases, there is a sudden onset of the short-range component of the nuclear interaction leading to a kink in the potential. Similar effects were observed at lower energies. The origin of the two-component potential is not clear. It warrants more theoretical investigation of the $\alpha$-$\alpha$ interaction.

The volume integrals of the real potential decrease linearly with increasing energy. This is in contrast to elastic $\alpha$-scattering from heavier nuclei, where the real potential volume integrals have a logarithmic dependence on the beam energy. This difference is attributed to the fact that the $\alpha$-particle is very tightly bound and there are very few reaction channels available. Finally, the data show no preference for a hard-core repulsive potential.

This work has been supported by the U.S. National Science Foundation under Grant Nos. PHY 9602869 (UM-Dearborn), PHY 9513924 (University of Maryland), PHY 9423659 (Oberlin College), PHY 9528844 (NSCL).

# REFERENCES


[1] P.D. Curry and D.W.L Sprung, Nucl. Phys. **A216**, 125 (1973).

[2] G.J. Wozniak, D.P. Stahel, J. Cerny, and W.A. Jelley, Phys. Rev. C **14**, 815 (1976).

[3] N. Anantaraman, C.L. Bennet, J.P. Draayer, H.W. Fulbright, H.E. Gove, and J. Toke, Phys. Rev. Lett. **35**, 1131 (1975); H. Yoshida, Phys. Lett. **47B**, 411 (1973).

[4] P.G. Roos, N.S. Chant, A.A. Cowley, D.A. Goldberg, H.D. Holmgren, and R.Woody III, Phys. Rev. C **15**, 69 (1977).

[5] T.A. Carey, P.G. Roos, N.S. Chant, A. Nadasen, and H.L. Chen, Phys. Rev. C **29**, 1273 (1984).

[6] A. Nadasen *et al.*, Phys. Rev. C **39**, 536 (1989); A. Nadasen *et al.*, *ibid.* **47**, 674 (1993); A. Nadasen *et al.*, *ibid.* **59**, 760 (1999).

[7] R.E. Brown and Y.C. Tang, Nucl. Phys. **A170**, 225 (1971).

[8] F.C. Barker, Aust. J. Phys. **22**, 293 (1969).

[9] V.G. Neudatchin, V.I. Kukulin, V.L. Korotkikh, and V.P. Korrenoy, Phys. Lett. **34B**, 581 (1971).

[10] N.P. Heydenberg and G.M. Temmer, Phys. Rev. **104**, 123 (1956).

[11] T.A. Tombrello and L.S. Senhouse, Phys. Rev. **129**, 2252 (1963).

[12] P.Darriulat, G. Igo, H.G. Pugh, and H.D. Holmgren, Phys. Rev. **137B**, 315 (1965).

[13] W.S. Chien and R.E. Brown, Phys. Rev. C **10**, 1767 (1974).

[14] A. Nadasen, P.G. Roos, B.G. Glagola, G.J. Mathews, and V.E. Viola Jr., Phys. Rev. C **18**, 2792 (1978).

[15] W. Czyz and L.C. Maximon, Ann. of Phys. **52**, 59 (1969).

[16] R.J. Glauber,*High Energy Physics and Nuclear Structure*, ed. G. Alexander (North-Holland, Amsterdam, 1967), pp. 311-338.

[17] P. Swan, Proc. Roy. Soc. **228**, (1955);Ann. of Phys. **48**, 455 (1968).

[18] J.C. Fong *et al.*, Nucl. Phys. **A262**, 365 (1976).

[19] G. Igo, L.F. Hansen, and T.J. Gooding, Phys. Rev. **131**, 337 (1963).

[20] G.F. Steyn *et al.*, Phys. Rev. C **54**, 2485 (1996).

## TABLES

| Energy (MeV) | V (MeV) | $r_0$ (fm.) | $a_0$ (fm.) | $W_v$ (MeV) | $r_w$ (fm.) | $a_w$ (fm.) | $V'$ (MeV) | $r'_0$ (fm.) | $a'_0$ (fm.) |
|---|---|---|---|---|---|---|---|---|---|
| 280 | 95.0 | 0.949 | 0.840 | 5.44 | 2.368 | 0.411 | 18.9 | 0.779 | 0.117 |
| 620 | 1.08 | 1.400 | 6.212 | 1.82 | 2.353 | 0.108 | 17.4 | 1.279 | 0.546 |

TABLE I. Optical model potential parameters for fits shown by solid lines in Figs. 1 and 2.

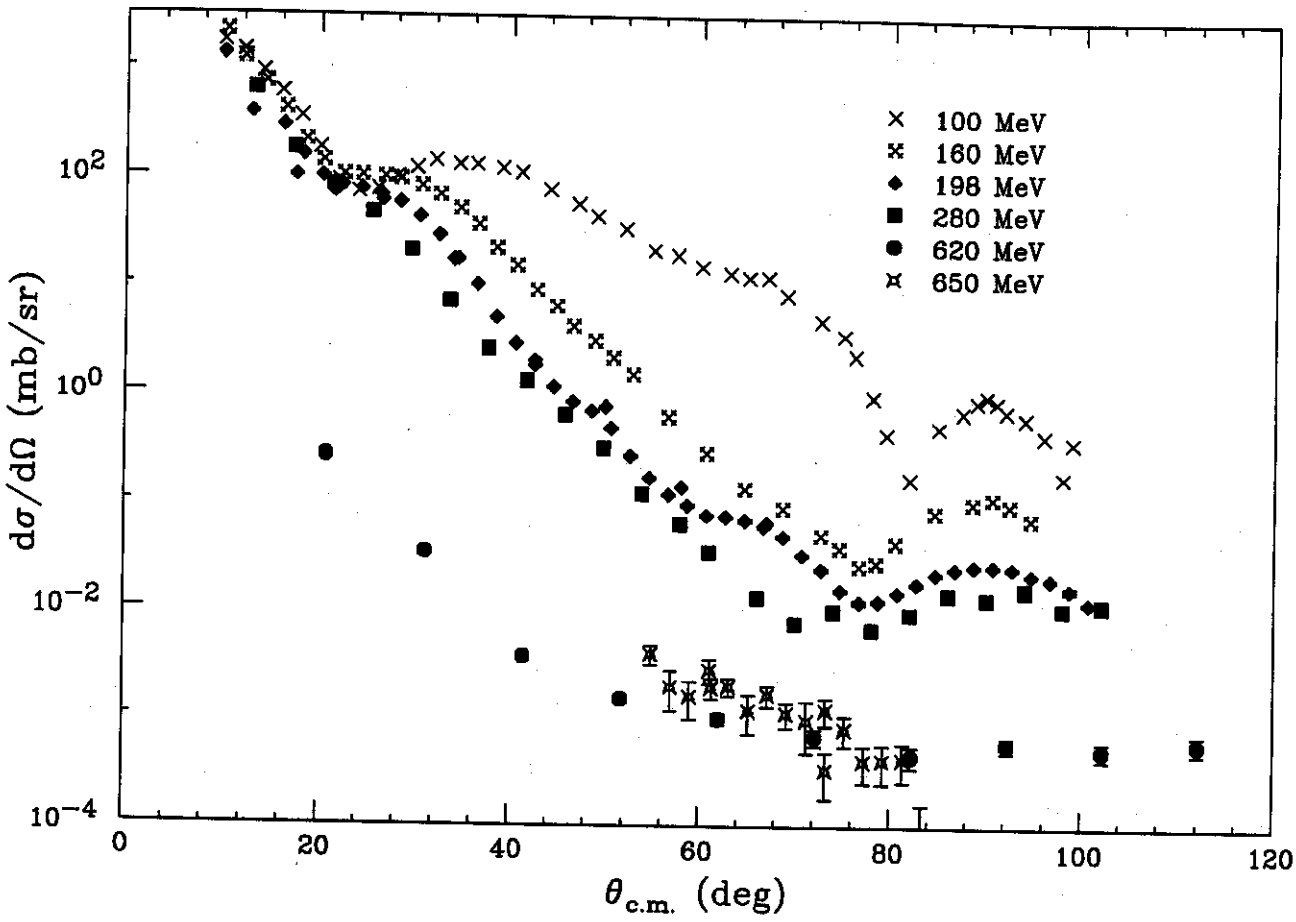


FIG. 1. Differential cross sections for $\alpha$-$\alpha$ elastic scattering at 280 MeV (solid squares) and 620 MeV (solid circles). Also included are available data from 100 to 650 MeV.

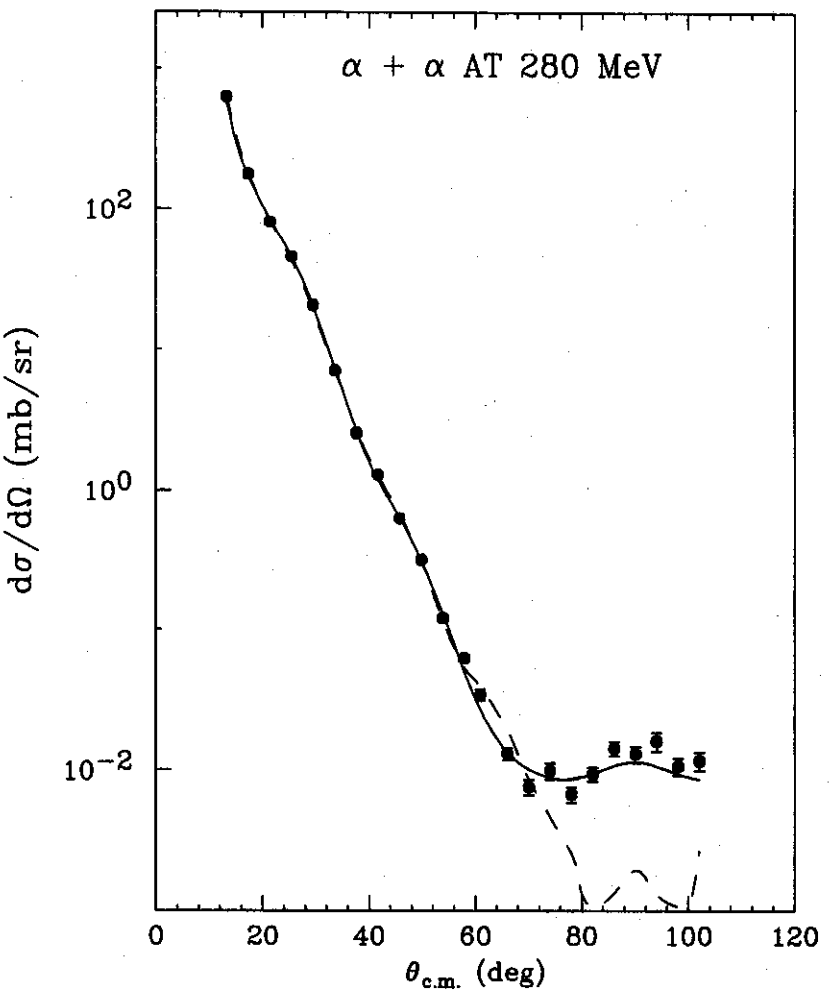


FIG. 2. Differential cross sections for the $\alpha$-$\alpha$ elastic scattering at 280 MeV. The nine-parameter optical model fit is shown by the solid line. The dashed line represents the six-parameter fit.

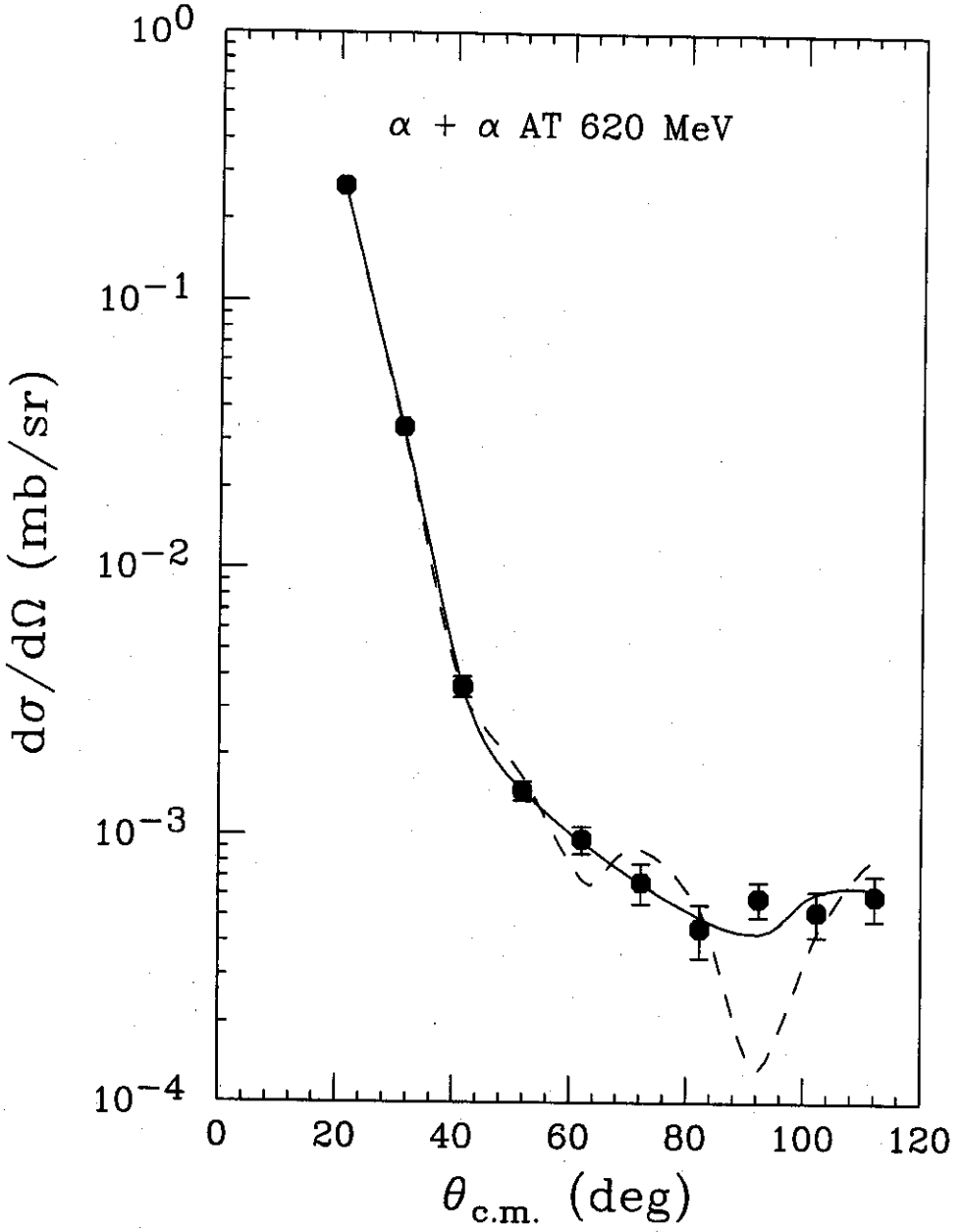


FIG. 3. Same as FIG.2 except for 620 MeV.

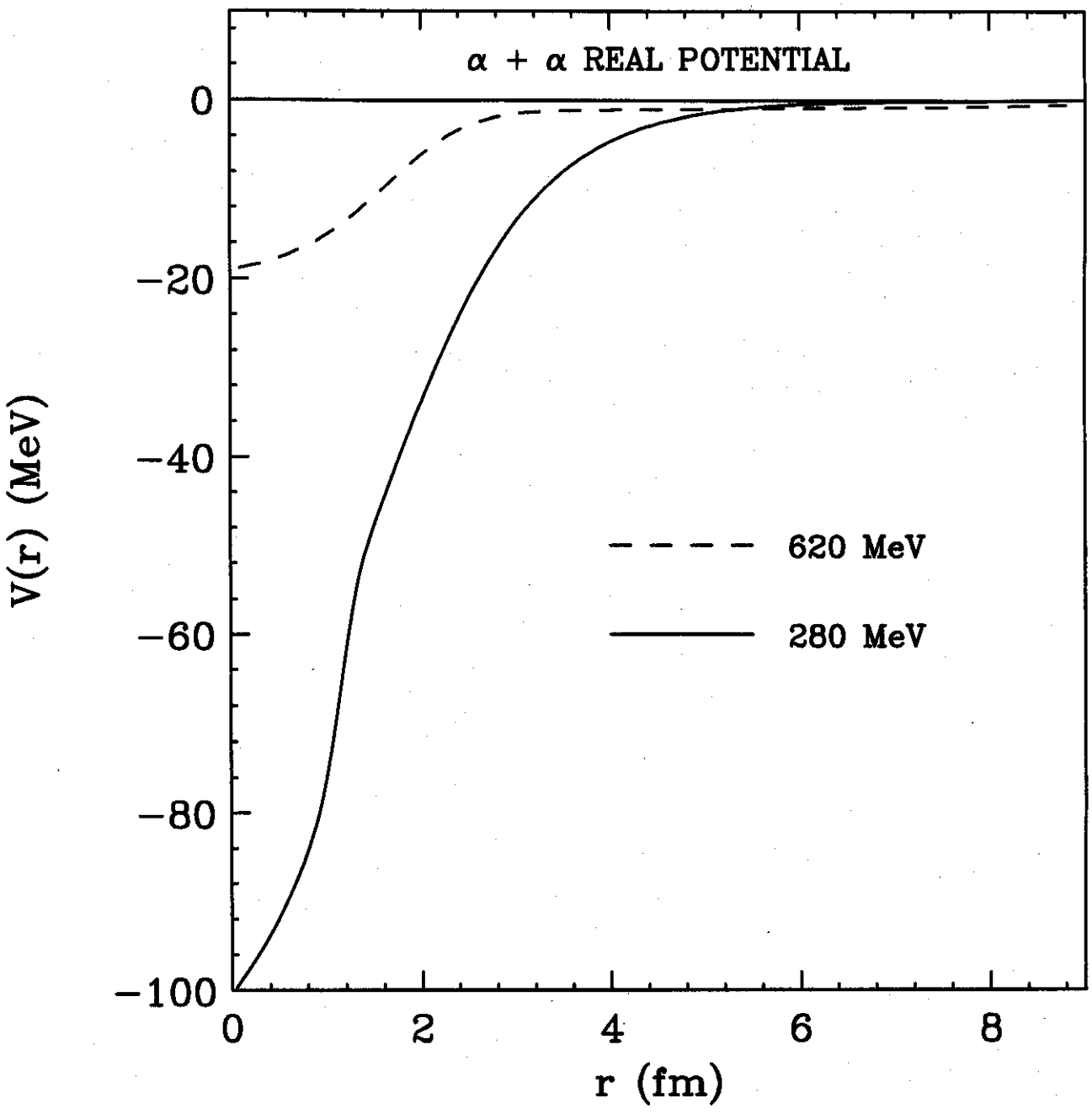


FIG. 4. The $\alpha + \alpha$ real potential at 280 and 620 MeV plotted as a function of radius.

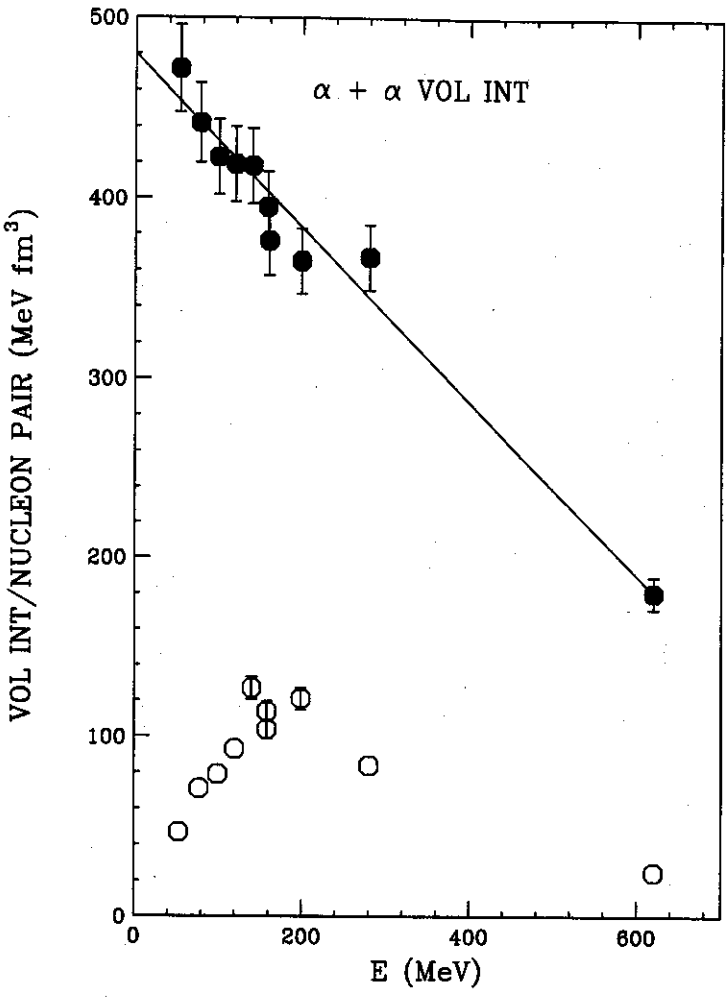


FIG. 5. The $\alpha + \alpha$ real (solid dots) and imaginary (open circles) potential volume integrals per nucleon pair (in MeV fm$^3$) plotted as a function of beam energy. 5% error bars have been assigned to the data points. The straight line is a least squares fit to the real potential volume integrals.